Dispersion-free pulse propagation in a negative-index material

Giuseppe D'Aguanno and Neset Akozbek

Time Domain Corporation, Cummings Research Park, 7057 Old Madison Pike, Huntsville, Alabama 35806

Nadia Mattiucci

Time Domain Corporation, Cummings Research Park, 7057 Old Madison Pike, Huntsville, Alabama 35806 and Departimento di Fisica "E. Amaldi," Università "RomaTre," Via Della Vasca Navale 84, I-00146 Rome, Italy

Michael Scalora and Mark J. Bloemer

Charles M. Bowden Research Center, Research, Development, and Engineering Command, Building 7804, Redstone Arsenal, Alabama 35898-5000

Aleksei M. Zheltikov

Department of Physics and International Laser Center, M. V. Lomonosov Moscow State University, Vorob'evy Gory, 119899 Moscow, Russian Federation

Received February 24, 2005

The possibility of controlling the spectral position of the zero group-velocity dispersion point of a negative-index material can be exploited by varying the ratio between the electric and the magnetic plasma frequency to obtain dispersion-free propagation in spectral regions otherwise inaccessible using conventional positive-index materials. Our predictions are confirmed by pulse propagation simulations where all the orders of the complex dispersion of the material are taken into account. © 2005 Optical Society of America

OCIS codes: 260.2030, 350.5500.

In the past few years, negative-index materials (NIMs), i.e., materials that have simultaneously negative electric susceptibility and magnetic permeability,[1] have been the subject of intense theoretical and experimental investigations.[2–5] Several applications have been envisioned for those materials. We cite, for example, the possibility of using them to construct a perfect lens, i.e., a lens that can also focus the evanescent near-field components of an object,[2] the possibility of exciting bright and dark gap solitons,[6] and the possibility of using a NIM as an efficient waveguide.[7] In this work we demonstrate that a NIM allows an ultrashort pulse to propagate with minimal dispersion due to the presence of a zero group-velocity dispersion (GVD) point.

Let us begin by describing the NIM with a lossy Drude model[2,6–8]: $\varepsilon(\tilde{\omega})=1-1/[\tilde{\omega}(\tilde{\omega}+i\tilde{\gamma}_e)]$, $\mu(\tilde{\omega})=1-(\omega_{\rm pm}/\omega_{\rm pe})^2/[\tilde{\omega}(\tilde{\omega}+i\tilde{\gamma}_m)]$, where $\tilde{\omega}=\omega/\omega_{\rm pe}$ is the normalized frequency, $\omega_{\rm pe}$ and $\omega_{\rm pm}$ are the respective electric and magnetic plasma frequencies, and $\tilde{\gamma}_e=\gamma_e/\omega_{\rm pe}$ and $\tilde{\gamma}_m=\gamma_m/\omega_{\rm pe}$ are the respective electric and magnetic loss terms normalized with respect to the electric plasma frequency. The refractive index n and the extinction coefficient δ of the material are given by $n+i\delta=\pm\sqrt{\varepsilon\mu}$. The sign in front of the square root must be chosen in a way that ensures the Poynting vector of the electromagnetic wave refracted into a semi-infinite slab of NIM will always be directed away from the interface into the refracting material itself.[6] In Fig. 1(a) we show refractive index n for different values of ratio $\omega_{\rm pm}/\omega_{\rm pe}$, and in Fig. 1(b) we show the GVD parameter $\beta_2=\mathrm{d}^2k/\mathrm{d}\omega^2$,[9] where $k=n\omega/c$ is the NIM wave vector. In our model we assume $\tilde{\gamma}_e\sim\tilde{\gamma}_m\sim10^{-4}$ and the extinction coefficient δ in the region around the zero GVD point is also of the order of 10^{-4}.

Note that the zero GVD points (i.e., the points where $\beta_2=0$) are located in the region where $\omega<\omega_{\rm pe}$ and that no zero GVD point is present when $\omega_{\rm pm}/\omega_{\rm pe}=1$. In Fig. 2 we show three snapshots of an unchirped, ultrashort, Gaussian pulse with its cen-

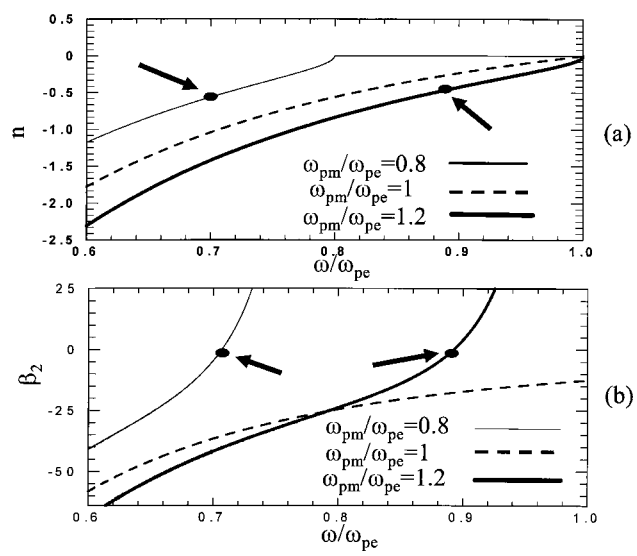

Fig. 1. (a) Refractive index n versus $\omega/\omega_{\rm pe}$ for different values of the ratio $\omega_{\rm pm}/\omega_{\rm pe}$: $\omega_{\rm pm}/\omega_{\rm pe}=0.8$ (thin solid curve), $\omega_{\rm pm}/\omega_{\rm pe}=1$ (dashed curve), $\omega_{\rm pm}/\omega_{\rm pe}=1.2$ (thick solid curve). (b) GVD parameter β_2 versus $\omega/\omega_{\rm pe}$ for different values of the ratio $\omega_{\rm pm}/\omega_{\rm pe}$. Note that the β_2 curves are plotted only in the region around their respective zero GVD points. The arrows indicate the position of the zero GVD points. β_2 is calculated in units of $\lambda_{\rm pe}/(4\pi^2c^2)$, where $\lambda_{\rm pe}=2\pi c/\omega_{\rm pe}$.

0146-9592/05/151998-3/$15.00

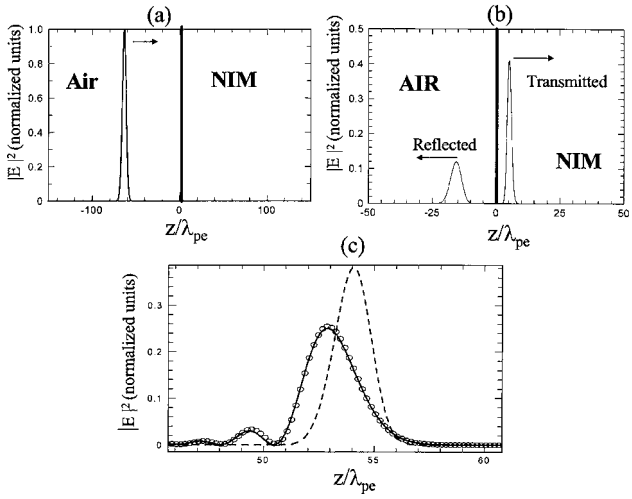

Fig. 2. Pulse propagation at different times of an ultrashort, Gaussian, unchirped pulse in a NIM at the zero GVD point for $\omega_{pm}/\omega_{pe}=0.8$. (a) At $t_0=0$, the pulse is in air directed toward the NIM, and $z=0$ is the air–NIM interface. The peak of the square modulus of the incident electric field is normalized to 1. Its FWHM is $\sim 5\lambda_{pe}$. (b) At $t_1=600\lambda_{pe}/(2\pi c)$, the incident pulse has entered the NIM giving rise to a reflected and a transmitted pulse. The FWHM of the transmitted field is $\sim 2\lambda_{pe}$. (c) At $t_2=1400\lambda_{pe}/(2\pi c)$, the transmitted pulse (thick solid curve) has propagated for approximately $50\lambda_{pe}$ in the NIM and its FWHM is $\sim 2.67\lambda_{pe}$. For comparison, the same pulse (dashed curve) at the same time after it has propagated in the same NIM but with the dispersion approximated up to the second order and with the dispersion approximated up to the third order (open circles).

tral frequency tuned at $\omega_c=0.706\omega_{pe}$ that corresponds to a zero GVD point for $\omega_{pm}/\omega_{pe}=0.8$, as shown in Fig. 1(b). In Fig. 2(a) the pulse is in air away from the air–NIM interface and its FWHM is $\sim 5\lambda_{pe}$; in Fig. 2(b) the pulse has entered the NIM, giving rise to a reflected and a transmitted field. $\lambda_{pe}=2\pi c/\omega_{pe}$ is the electric plasma wavelength, and c is the velocity of light in vacuum. Note that the transmitted pulse is now spatially compressed with a FWHM of $\sim 2\lambda_{pe}$ while its temporal duration shortly after it has entered the medium is $T\sim 2\lambda_{pe}/V_g\sim 5.8\lambda_{pe}/c$, where $V_g\sim 0.34c$ is the group velocity of the pulse. In Fig. 2(c) we show the transmitted pulse after it has propagated in the NIM for ~ 25 times its FWHM width, i.e., $\sim 50\lambda_{pe}$. The pulse maintains a FWHM of less than $3\lambda_{pe}$. The ripples that appear on the left of the main pulse and the slight increase in the FWHM are due mostly to third-order dispersion. In our calculations all the dispersion orders are taken into account.[10]

In Fig. 2(c) we also show the pulse at the same time after it has propagated in the same NIM except that now the complex wave vector of the NIM, $\hat{k}(\omega)=(n+i\delta)(\omega/c)$, is approximated up to second order (dashed curve) around the central frequency of the pulse and up to third order (open circles). In the case of second-order dispersion only, the pulse propagates undistorted and with no dispersion, as expected. A small decrease in the amplitude of the undistorted pulse with respect to the amplitude of the incident pulse [see Fig. 2(b)] is due to linear absorption. On the other hand, taking dispersion terms up to third order produces a pulse almost identical in shape and amplitude to the pulse obtained via the exact calculation. The high-order dispersion length, $L_D^{(3)}=T_0^3/|\beta_3|$, gives an estimate of the propagation distance over which the cubic dispersion term starts to play a significant role[9]; T_0 is a measure of the initial pulse duration in time, and $\beta_3=d^3k/d\omega^3$. In the case depicted in Fig. 2 $T_0\sim 5\lambda_{pe}/c$, and $d^3k/d\omega^3\sim 700\lambda_{pe}^2/(8\pi^3c^3)$, giving a dispersion length of $L_D^{(3)}\sim 40\lambda_{pe}$, consistent with the results of our numerical calculation. In Fig. 3 the central frequency of the pulse is now tuned at $\omega_c=0.892\omega_{pe}$, which corresponds to the zero GVD point when $\omega_{pm}/\omega_{pe}=1.2$. The incident pulse has the same duration in time of that shown in Fig. 2(a), i.e., $T_0\sim 5\lambda_{pe}/c$. The calculated high-order dispersion length is now $L_D^{(3)}\sim 60\lambda_{pe}$, which is longer than that of the previous case; this is consistent with the results of our numerical calculation [see Fig. 3(c)].

In principle, the use of longer pulses would give rise to a much longer dispersion length: For example, the use of a pulse of time duration $T_0\sim 5\times 10^3\lambda_{pe}/c$ would make the dispersion length longer by a factor of 10^9 than those previously calculated, and therefore the pulse could propagate undistorted and with no dispersion for a distance of approximately $10^{10}\lambda_{pe}$. Moreover the dependence of the position of the zero GVD points on the electric and magnetic plasma frequency might open the door to a whole new class of artificial materials assembled in such a way as to obtain dispersion-free propagation in spectral regions otherwise inaccessible for conventional positive-index materials. In photonic crystal fibers[11] or in tapered fibers,[12] for example, the tunability of the zero

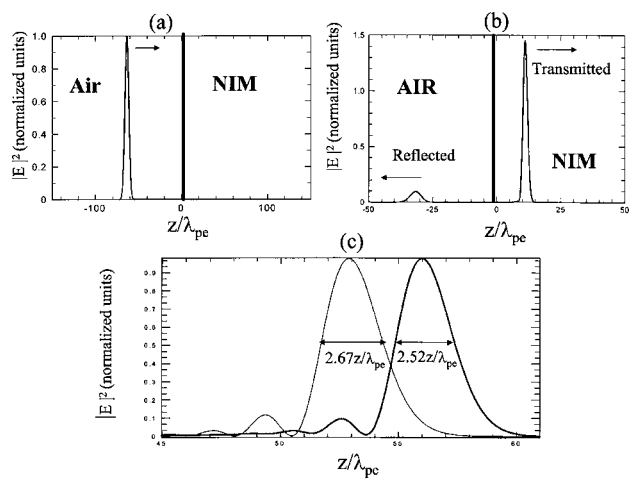

Fig. 3. Pulse propagation in a NIM at the zero GVD point for $\omega_{pm}/\omega_{pe}=1.2$. (a) Incident pulse at $t_0=0$. (b) Transmitted and reflected fields at $t_1=600\lambda_{pe}/(2\pi c)$. (c) Transmitted pulse (thick solid curve) at $t_2=1400\lambda_{pe}/(2\pi c)$. For comparison, we also plot the transmitted pulse calculated in Fig. 2(c) (thin solid curve in the present figure) but with its amplitude renormalized to the amplitude of the pulse calculated in this case.

GVD point has been demonstrated within the entire visible range. In contrast, NIMs offer the possibility of tuning the zero GVD zone in a quite different spectral range that spans from the microwave to the near-infrared range. In Ref. 3, for example, a NIM was fabricated and experimentally tested in the microwave range, while the experimental results reported in Ref. 5 point toward the possibility of having a NIM operating in the near-infrared regime. However, although at least in principle dispersion-free propagation in NIMs is possible, the issue of absorption and/or loss is still a serious obstacle to its practical realization. In our model the extinction coefficient is of the order of 10^{-4}, corresponding to an attenuation length of several hundreds of wavelengths in units of λ_{pe}. This means that, for example, a pulse of temporal duration $T_0 \sim 5 \times 10^2 \lambda_{pe}/c$ will be attenuated by a factor of $1/e$ after it has propagated for only approximately one FWHM. Currently available metamaterials experimentally tested have an even shorter attenuation length: ~10 wavelengths or less.[3] It is interesting to note that absorption represents a limiting factor also in the case of the so-called superlensing effect.[2] On the other hand, while the causality principle requires that the real and imaginary parts of the dispersion of a medium be Kramers–Kronig pairs, it does not put a limit on how small the absorption of a medium should be, as long as it is not zero. The real and imaginary parts of both ε and μ in our lossy Drude model are in fact Kramers–Kronig pairs regardless of how small the electric and magnetic loss terms may be. Therefore, although NIMs with low absorption are at the present time out of reach, nevertheless, in principle, nothing prevents their availability in the near future.

G. D'Aguanno's e-mail address is giuseppe.daguanno@timedomain.com.

References

1. V. G. Veselago, Sov. Phys. Usp. **10**, 509 (1968).
2. J. B. Pendry, Phys. Rev. Lett. **85**, 3966 (2000), and references therein.
3. R. A. Shelby, D. R. Smith, and S. Schultz, Science **292**, 77 (2001).
4. C. G. Parazzoli, R. B. Greegor, K. Li, K. E. C. Koltenbah, and M. Tanielian, Phys. Rev. Lett. **90**, 107401 (2003).
5. S. Linden, C. Enkrich, M. Wegener, J. Zhou, T. Koschny, and C. M. Soukoulis, Science **306**, 1351 (2004).
6. G. D'Aguanno, N. Mattiucci, M. Scalora, and M. J. Bloemer, Phys. Rev. Lett. **93**, 213902 (2004).
7. G. D'Aguanno, N. Mattiucci, M. Scalora, and M. J. Bloemer, Phys. Rev. E **71**, 046603 (2005).
8. R. W. Ziolkowski, Phys. Rev. E **70**, 046608 (2004), and references therein.
9. G. P. Agrawal, *Nonlinear Fiber Optics* (Academic, 1995).
10. The electric field was calculated as follows: $E(z,t) = \int_{-\infty}^{+\infty} E(0,\omega)\exp(-i\omega t)[\exp(i\omega z/c) + r(\omega)\exp(-i\omega z/c)]\mathrm{d}\omega$ for $z<0$ and $E(z,t) = \int_{-\infty}^{+\infty} t(\omega)E(0,\omega)\exp\{i[\hat{k}(\omega)z - i\omega t]\}\mathrm{d}\omega$ for $z>0$, where $r(\omega)$ and $t(\omega)$ are, respectively, the reflection and transmission coefficient of the air–NIM interface, $E(0,\omega)$ is the spectral amplitude of the incident pulse, and $\hat{k}(\omega)$ is the complex wave vector of the NIM.
11. P. St. J. Russell, Science **299**, 358 (2003), and references therein.
12. R. Zhang, J. Teipel, X. Zhang, D. Nau, and H. Giessen, Opt. Express **12**, 1700 (2004), and references therein.